

Feasibility of Single-Scan Material Decomposition for Dedicated Breast CT: A Phantom Study

Bitbyeol Kim^a, Ho Kyung Kim^a, Hosang Jeon^{b*}

^a School of Mechanical Engineering, Pusan National University, Busan, Republic of Korea

^b Department of Radiation Oncology, Pusan National University Yangsan Hospital,
Yangsan, Gyeongsangnam-do 50621, Republic of Korea,

*Corresponding author: hjeon316@gmail.com

1. Introduction

Despite the observed reduction of mortality from breast cancer in the last 25 years, Breast cancer is the second most common cancer and the most frequent cause of women death from cancer in the world [1]. Early detection with imaging is considered one of the main causes for reduction therefore accurate breast imaging is required. Although mammography of compressed breast is considered as the gold standard for detection, all breast cancers are not detected with mammography. Contrast material-enhanced breast magnetic resonance imaging is the most sensitive imaging modality [2], but it is practical only for high-risk groups because of high cost and access limitation. Breast computed tomography (BCT) is an emerging technique that has been actively studied in recent year [3,4]. BCT has a three-dimensional (3D) imaging modality which could improve diagnostic accuracy.

In this study, we proposed a single-energy single-scan (SESS) material decomposition method for BCT and evaluated the image quality. In addition, our result was compared with conventional single-energy CT images.

2. Methods and Results

2.1 Theory

A projection image acquired by an X-ray imager is related to the linear attenuation coefficient that is a function of material and photon energy, and the beam penetration length within the imaging object. The penetration path length toward the corresponding pixel on the projection image can be calculated using a ray-tracing method [5] by the following:

$$L_i(x, y) = \sum l_i(p, q, r)$$

where l_i is the X-ray path length penetrating a voxel of i th basis material in (p, q, r) position toward (x, y) detector pixel, and L_i is the sum of all l_i values. The l_i depends on the geometric parameters of the CBCT system, such as distance and angle from the ratio of source-to-image distance (SID) and source-to-axis distance (SAD) and

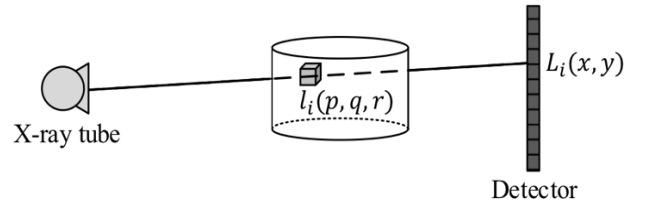


Figure 1. A schematic drawing of the beam penetration path length

the number of detector pixels, and reconstructed voxel size. This system is shown in Figure 1.

Assuming that the object consists of two basis materials, the acquired projection image $I(x, y)$ can be expressed using Beer's law as:

$$\ln\left(\frac{I_0(x, y)}{I(x, y)}\right) = \mu_1 \cdot L_1(x, y) + \mu_2 \cdot L_2(x, y)$$

where $I_0(x, y)$ is an acquired image when the object is absent, and μ_i is the linear attenuation coefficient of i th basis material. The total penetration length $L_t(x, y)$ is simple calculated as below:

$$L_t(x, y) = L_1(x, y) + L_2(x, y)$$

Therefore, the beam penetration length for two basis materials can be calculated separately:

$$\begin{bmatrix} L_1(x, y) \\ L_2(x, y) \end{bmatrix} = \begin{bmatrix} \mu_1 & \mu_2 \\ 1 & 1 \end{bmatrix}^{-1} \begin{bmatrix} \ln(I(x, y)/I_0(x, y)) \\ L_t(x, y) \end{bmatrix}$$

Reconstructing L_i images, it is possible to obtain i th basis material selective image. Therefore, material enhanced image $I_M(x, y)$ is able to be obtained with calculated X-ray path and obtained projection image:

$$\ln\left(\frac{I_M(x, y)}{I_0(x, y)}\right) = \mu_m \cdot L_m(x, y)$$

where m is the basis material.

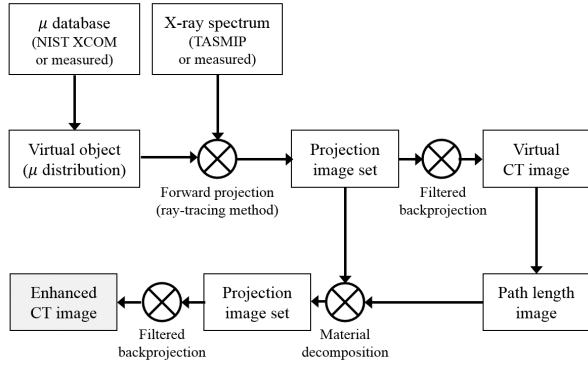


Figure 2. Scheme for single-energy material decomposition simulation with a virtual phantom.

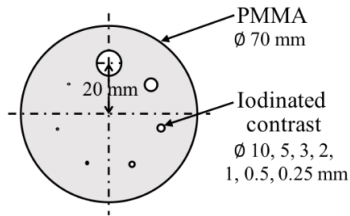


Figure 3. A virtual disk phantom including iodinated contrast for breast simulation

Table I: Simulation parameters

| | | |
|--------------|--------------------------------|-----------|
| X-ray source | Tube voltage (kV) | 60 |
| | Anode | Tungsten |
| | Added filter (mm) | 1.5 Al |
| | Beam shape | Cone-beam |
| Detector | Pixel pitch (mm) | 0.099 |
| | Active area (mm ²) | 100 X 150 |
| Geometry | Magnification | 1.88 |

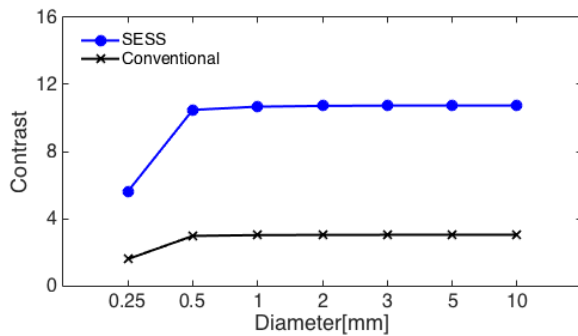


Figure 4. Image contrast between iodinated contrast and background

2.2 Image acquisition

To prove feasibility of the method, simulations were conducted with in-house Matlab program. A scheme for SESS method is illustrated in Figure 2.

The breast is modeled as an acrylic cylindrical phantom having slots with diameters of 0.25, 0.5, 1, 2, 3, 5, 10 mm. The slots are filled by iodinated contrast. Details of the phantom are illustrated in Figure 3.

Projection images of the phantom are obtained using a CBCT system composed of an X-ray tube with a tungsten anode and a flat-panel detector. The details of the parameters are tabulated in Table 1.

To acquire conventional and SESS CT images, the Feldkamp-Davis-Kress (FDK) algorithm which is typical for CBCT reconstruction was employed. The FDK algorithm is 3D approximation of 2D filtered backprojection (FBP) algorithm of conventional fan-beam CT imaging. It was introduced to reconstruct volumetric images from cone-beam projections [7]. The CBCT images consist of 800 X 800 pixels with a pixel size of 1.2 mm. In this study, attenuation coefficients are calculated from projection images of basis material phantom.

2.3 Image analysis

The purpose of this study is to enhance the micro-calcification for better detectability. Therefore, we measured the image contrast as indicator for image quality. To compare SESS images with conventional CT images, we conduct measurement within the regions of interest (ROIs) in the SESS images and corresponding CT images, respectively. The contrast was calculated using:

$$\text{Contrast} = \frac{\overline{I_{ROI}} - \overline{I_{bgn}}}{\overline{I_{bgn}}}$$

where I_{ROI} and I_{bgn} denote the mean image intensities of the ROIs and region of background, respectively.

3. Preliminary results

Preliminary calculations were conducted on simulation excluding scatter. The results are shown in Figure 3. In SESS images, iodinated contrast regions are successfully enhanced as the contrast is improved by a factor of 3.532 – 3.547.

4. Ongoing and Further Studies

To verify practical feasibility, experimental image acquisition will be carried out.

In addition, the contrast-to-noise ratio (CNR) which contains noise factor of the image also measured because of the probability that proposed method might increase the image noise due to image synthesis.

ACKNOWLEDGEMENT

This work was supported by the National Research Foundation of Korea (NRF) grants funded by the Korea governments (MSIP) (No.2015M3A9E2067002, No. 2017M2A2A6A01071267)

REFERENCES

- [1] http://globocan.iarc.fr/Pages/fact_sheets_cancer.aspx. GLOBOCAN Cancer facts sheets: Breast cancer. Lyons, France: International Agency for research on Cancer; 2012. Accessed online on 15/1/2017
- [2] C. D. Lehman, J. D. Blume, P. Weatherall, D. Thickman, N. Hylton, E. Warner, E. Pisano, S. J. Schnitt, C. Gatsonis and M. Schnall "Screening Women at High Risk for Breast Cancer with Mammography and Magnetic Resonance Imaging," *Cancer*, 103(91), 2005
- [3] K. K. Lindfors, J. M. Boone, T. R. Nelson, K. Yang, A. L. C. Kwan, and D. F. Miller, "Dedicated breast CT: Initial Clinical Experience," *Radiology*, 246(3), 2008
- [4] W. T. Yang, S. Carkaci, L. Chen, C. Lai, A. Sahin, G. J. Whitman, and C. C. Shaw, "Dedicated cone-beam breast CT: Feasibility study with surgical mastectomy specimens," *American Journal of Roentgenology*, 189, 1312-1315, 2007
- [5] R. L. Siddon, "Fast calculation of the exact radiological path for a three-dimensional CT array," *Medical Physics*, 12(2), 1985
- [6] S. V. Dorozhkin and M. Epple, "Biological and Medical Significance of Calcium Phosphates," *Angewandte Chemie International Edition*, 41: 3130-3146, 2002
- [7] L.A. Feldkamp, L. C. Davis, and J. W. Kress, "Practical cone-beam algorithm," *Optical Society of America*, 1(6), 1984